JOURNAL OF OPTOELECTRONICS AND ADVANCED MATERIALS Vol. 9, No. 6, June 2007, p. 1808 - 1812

Magnetoresistive sensors based on AMR and GMR effects for biomedical applications

M. VOLMER, M. AVRAM[a]
Physics Department, Transilvania University, 29 Eroilor, Brasov 500036, Romania
[a]National Institute for Research and Development in Microtechnologies,
Str. Erou Iancu Nicolae 32B, 72996 Bucharest, Romania

Structures as $Ni_{80}Fe_{20}/Cu/Ni_{80}Fe_{20}$ were used to build high sensitivity magnetic field sensors. We discuss, in this paper, the micromagnetic behaviour of these structures for two sensing applications: (i) a micro compass for detection of the position and rotation rate of a micro rotor used to study the dynamics of the biological fluids and (ii) a detection system of the magnetic particles employed in biology as markers or as carriers for targeted drug delivery. The coupling between the magnetic particles and the measurement system was also considered. The designing process for experimental measurements was made using the NI ELVIS prototyping environment.

(Received November 14, 2006; accepted April 26, 2007)

Keywords: Thin Films, Giant magnetoresistance (GMR), Planar Hall effect, Magnetic detection

1. Introduction

Lab-on-a-chip devices shrink entire chemical or biochemical assays down to small microfluidic chips. There are several systems used for biological fluids flow and viscosity measurements. A micro-electro-mechanical system (MEMS) consisting of a gear wheel and magnetoresistive sensors is proposed for biological fluids flow and viscosity measurements. The gear wheel was fabricated using the silicon surface micromachining technology. On this gear can be deposited 1 or 2 micromagnets which are used to produce the magnetic field to be detected by the sensors. The physical arrangement and the electrical Wheatstone bridge configuration are illustrated in Fig. 1. The sensing resistors are located between flux concentrators in order to increase the sensibility and to minimize the influence of the external fields.

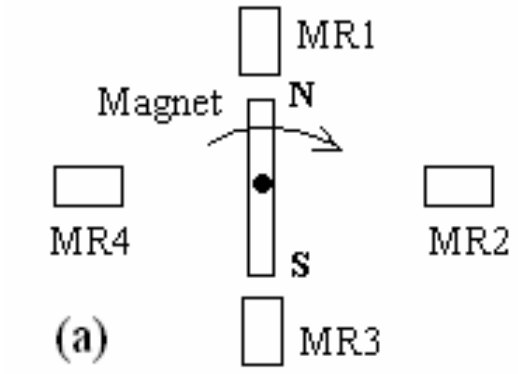

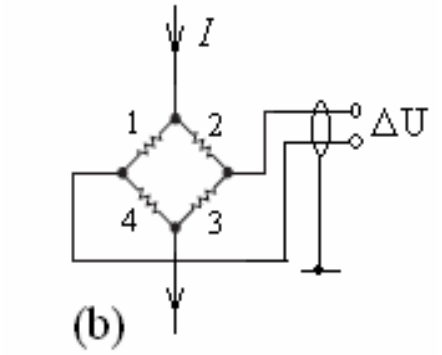

Fig. 1. (a) The schematic structure of the rotation sensor with magnetoresistors and (b) the Wheatstone bridge configuration with GMR sensors according to the setup presented in (a).

All resistors are multilayered structures $Si/SiO_2/[NiFe(2\ nm)/Cu(1\ nm)]_{12}$ deposited in a sputtering system at 200 W and 30 mTorr, Ar pressure. Between the Permalloy layers there is an oscillatory exchange coupling through the Cu layers. When the thickness of the Cu layer is 0.85 nm there is a strong antiferromagnetic coupling between the adjacent Permalloy layers but also the saturation field increases to 1000 Oe. For 1 nm thickness of the Cu layer the AF coupling is lower and the saturation field decreases to about 250 Oe as it was reported also in [1]. The GMR amplitude is about 2 % which is acceptable for this application.

Because MR sensors made with magnetic layers are sensitive for small magnetic fields, they are very attractive for lab-on-a chip applications used for biological diagnostics. This application includes detection of small magnetic fields generated by magnetic particles

encapsulated in plastic, carbon or ceramic spheres which are coated with chemical or biological species such as DNA or antibodies that selectively binds to the target analyte. Results from theoretical modelling, as well as laboratory tests, show that GMR detectors can resolve single micrometer-sized magnetic beads. Figure 2 shows, in a simple view, the bonding of the beads to the sites – GMR sensor - via the molecules to be detected (antigens, in our example). Several bioassays can be simultaneously accomplished using an array of magnetic sensors, each with a substance that bonds to a different biological molecule. This application requires extremely small, low-power, low field magnetic sensors.

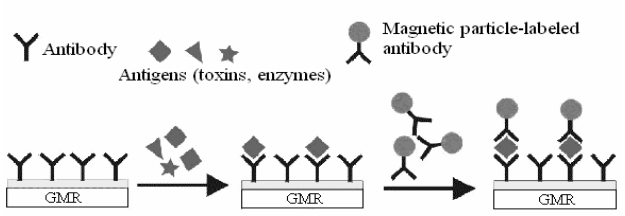

Fig. 2. Antigens are detected by flowing them over a sensor coated with antibodies to which they bind. The magnetic particle-labeled antibodies then bind to the antigens providing a magnetic indication of the presence of those antigens.

The magnetic microbeads will be coated with the materials to be analyzed. The microbeads in suspension were allowed to settle onto the GMR sensor array where specific beads bonded to specific sensors only if the materials were designed to attract each other. Nonbinding beads can be removed by a small magnetic field. The beads are then magnetized by a dc or an ac electromagnet and detected by the GMR sensors. The microbeads are made up of nm sized iron oxide particles that have little or no magnetization in the absence of an applied field.

2. Results and discussion

2.1. The response analysis of the rotation sensor

We used a micromagnetic simulator, SimulMag [2], to obtain the response of the magnetoresistive sensors which transform the rotation of a micromagnet attached to a rotor into an electrical signal. This is an application for biological fluids flow and viscosity measurements. The sensitive structure uses a full Wheatstone bridge configuration with four active GMR elements, as presented in Fig. 1. In our simulations, the magnet, attached to the rotor, has a length of 4 μm and a width of 1 μm. The thickness of the micromagnet is 0.4 μm. The dimensions of the GMR sensors are 3x1x0.05 μm^3. These dimensions are inspired from the real structures that are designed and will be manufactured at the National Institute for Research and Development in Microtechnologies, Bucharest. We assumed a uniaxial anisotropy direction perpendicular to the long dimension of the sensor i.e. perpendicular to the applied magnetic field. In this way the hysteresis effects can be lowered. If we consider the starting point, see Fig. 1(a), when the magnet is in the front of sensors 1 and 3, we obtained by micromagnetic simulations the angle dependencies of the magnetization, M, and the electrical resistance, R_1, of the sensor GMR1, presented in Fig. 3(a) and Fig. 3(b) respectively. In Fig. 3(c) we present a picture taken during the micromagnetic simulation. We can see how the magnetic moments of the sensor GMR1 are oriented antiparallel when the magnetic field applied to this sensor is zero and how the magnetic moments for the sensor GMR2 tends to have the orientation, given by the applied magnetic field. This means that the resistance R_1 will have the maximum value whereas R_2 will have a minimum. Because the GMR effect is defined by

$$GMR = \frac{R_{AP} - R_P}{R_P} \tag{1}$$

the evolution of the electrical resistance gives the evolution of the GMR effect

Here, R_P denotes the minimum value of the resistance obtained when the magnetizations from the ferromagnetic layers are all parallel and R_{AP} denotes the maximum value of the resistance which appears when the magnetizations from the adjacent magnetic layers are antiparallel.

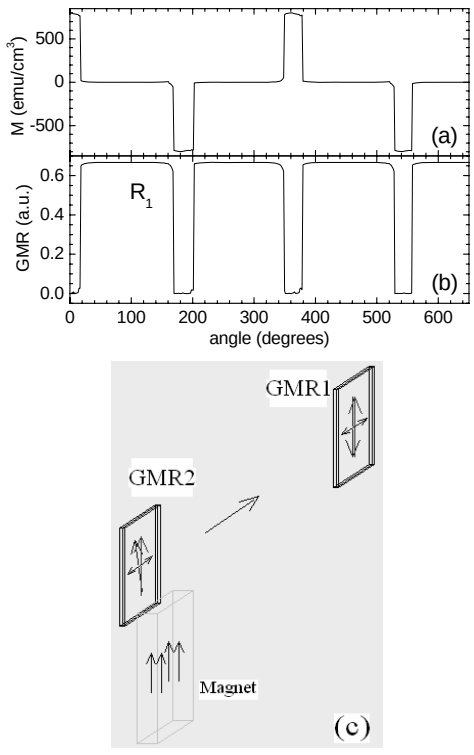

Fig. 3. The angular dependence of the magnetization (a) and GMR effect (b) for the sensor GMR1. The image taken during the micromagnetic simulation shows the orientation of the magnetizations in sensors GMR1 and GMR2 and the orientation of the uniaxial anisotropy.

We see from Fig. 3 the correlation between the magnetization and GMR effect. Because of the sensors position and because the GMR effect is an even effect, the angular dependencies for the sensors GMR1, GMR3 and GMR2, GMR4 will be the same. Using this approach we have simulated the angular response of the Wheatstone bridge when the micro-magnet is rotated in a clockwise direction. The angular dependencies of the GMR effect for resistors R_1 (R_3) and R_2 (R_4) are presented in Fig. 4(a) and Fig. 4(b) respectively.

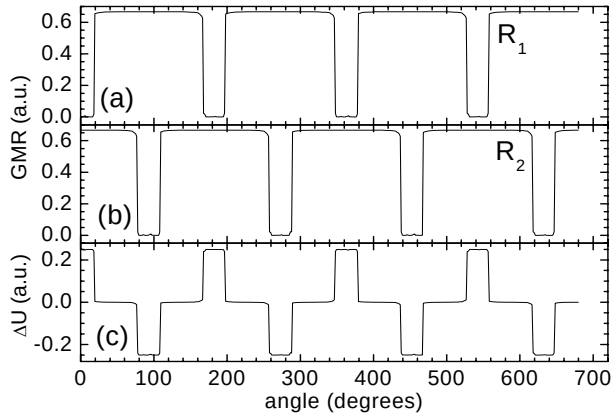

Fig. 4. The micromagnetic simulation of the GMR behaviour of the resistors from the Wheatstone bridge; ΔU denotes the output of the bridge.

The response of the bridge is presented in Fig. 6(c) and illustrates how does work the rotation sensor with GMR elements.

2.2 Detection of magnetic particles in biological applications

In this subsection we describe the detection of magnetic beads labeled with different biological structures. Magnetic micro-beads when magnetized by an external field have a magnetic dipole field as we sketched in Fig. 5. This field is proportional to the volume of magnetic material and inversely proportional to the distance cubed. So, detecting these small fields is increasingly difficult as the distance from the bead to the sensor increases. On the other hands, if the sensitive area is much larger than the bead, only the portion of the magnetoresistive material close to the bead will be affected. Therefore the fractional change in resistance, and hence the sensitivity, will be maximized by matching, if is possible, the size of the sensor to the size of the bead and by reducing the distance between the sensor and the bead. This requirement matches the attributes of GMR sensors [3].

The amplitude of stray fields produced by the beads depends on the nature and particle dimension. In our simulations regarding the sensor response we'll assume a total thickness of the layers (immobilization layer and protection layer – Si_3N_4) between the bead and the GMR sensor of 0.2 μm. The sensor dimensions are 1x1x0.1μm^3. The bead is assumed to be a cube with a side of about 0.2 μm. The saturation magnetization of the micro-magnetic bead is 400 emu/cm^3. For an external magnetic field of 500 Oe, the amplitude of the stray field in the sensor region, under the above conditions, is between 8 and 24 Oe.

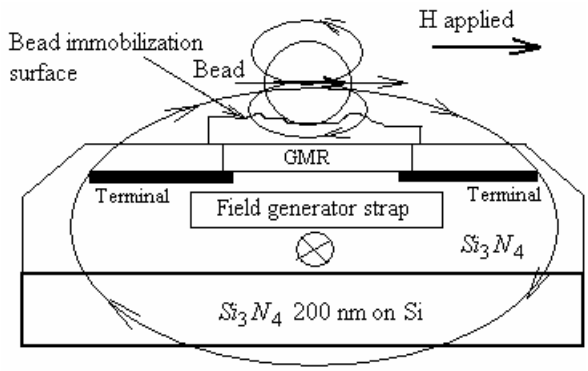

Fig. 5. The schematic setup for a GMR sensor that detects the stray field generated by a bead. The field that magnetizes the immobilized bead can be generated by a strap located beneath the sensor.

In order to extract the contribution corresponding to the total magnetic moment of the bead and to avoid the influence of the external magnetic fields and thermal variations we designed a differential measurement system like in Fig. 6. The driving voltage, U_C, sets constant currents, $I_1=U_C/R_1$, $I_2=U_C/R_2$, through the sensors GMR1 and GMR2. From basic electronics, we have for the output voltage that is applied to the data acquisition system the expression (in modulus):

$$\Delta U = \left(U_{GMR1} + U_C\right) - \left(U_{GMR2} + U_C\right) = \\ = U_{GMR1} - U_{GMR2} = f\left(H_{bead}\right) \quad (2)$$

where H_{bead} denotes the strength of the stray field generated by the magnetic bead in the sensor region.

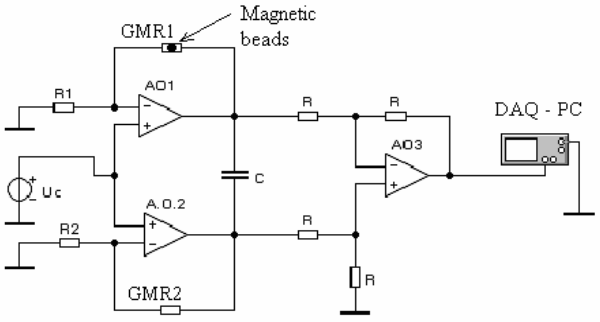

Fig. 6. The differential measurement setup used to measure the stray field produced by the magnetic bead.

The micromagnetic simulations for a differential measurement system, according to physical and electronic setup shown in Figs. 5-6, are presented in Fig. 7(a) when the magnetic field is applied parallel to the easy axis and in Fig. 7(b) when the magnetic field is applied perpendicular to the easy axis. The results show only the contribution of the stray fields produced by the micro-

bead. The output, ΔU, of the differential amplifier, plotted in Fig. 7, is directly proportional to the changes of the GMR amplitude that takes place in the sensor GMR1 due to the presence of the micro-bead at 200 nm above.

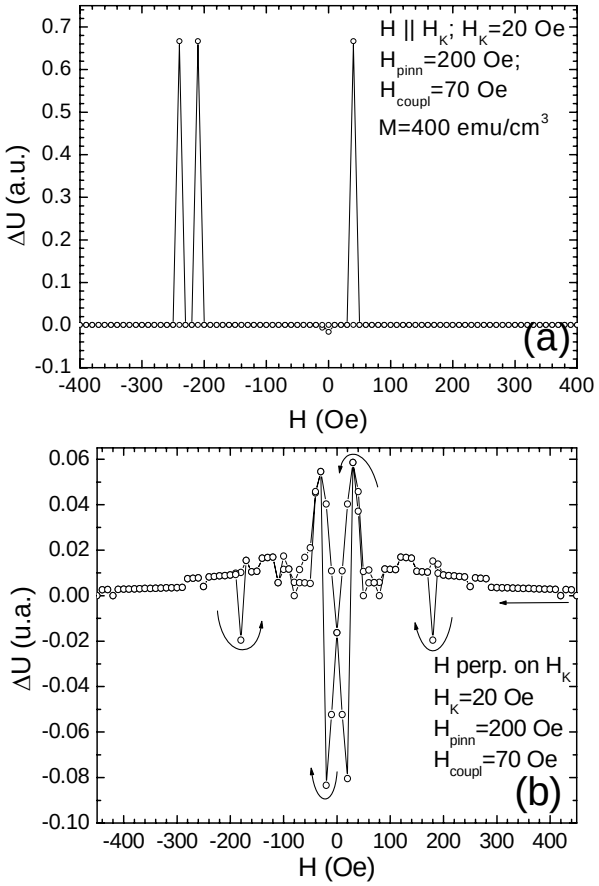

Fig. 7. The response of a differential system with GMR sensors for a magnetic micro-bead placed 200 nm above the sensor GMR1, when the magnetic field is applied (a) parallel and (b) perpendicular to the easy axis. The sensor GMR2 is used as reference. The arrows are guide for the eyes.

In these simulations the GMR sensors consist of multilayer structures as FeMn/NiFe(2 nm)/Cu(1 nm)/NiFe(2 nm) for which we assumed a small positive coupling between the magnetic layers through the nonmagnetic layer, H_{coupl}=70 Oe and a uniaxial anisotropy field H_K=20 Oe. This positive coupling is often present in real structures due to the small iregularities of the surfaces giving the so called orange-peel coupling [4]. In order to obtain the GMR effect in these structures, the magnetization of bottom layer is pinned by exchange interaction, using a layer of FeMn. The bead is placed above the free layer. The amplitude of the ΔU(H) plots and positions of the peaks depend on the volume and magnetic moment of the micro-beads. For this reason the best detection method is to sweep the magnetic field between the limits illustrated in Fig. 7, i.e. to perform a complete magnetization curve. Using alternating magnetic fields it is possible to compensate the thermal drift of the sensors and electronics and the structure temperature remains at low values avoiding the damaging of the biological fluids.

Another method to measure the magnetic field produced by the micro-beads is to use a full Wheatstone bridge in which all the resistors are GMR elements subjected to the same external magnetic field, *H*. The magnetic particles will be located between two sensors, GMR1 and GMR2, placed in opposite branches of the bridge, as in Fig. 8.

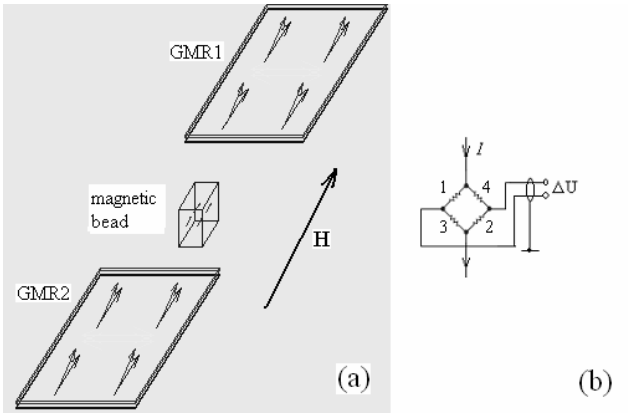

Fig. 8. The measurement setup (a) and the electrical connection of the sensors (b).

Using the same data for sensors and magnetic bead the micromagnetic simulations give us the response of the measurement circuit, presented in Fig. 9.

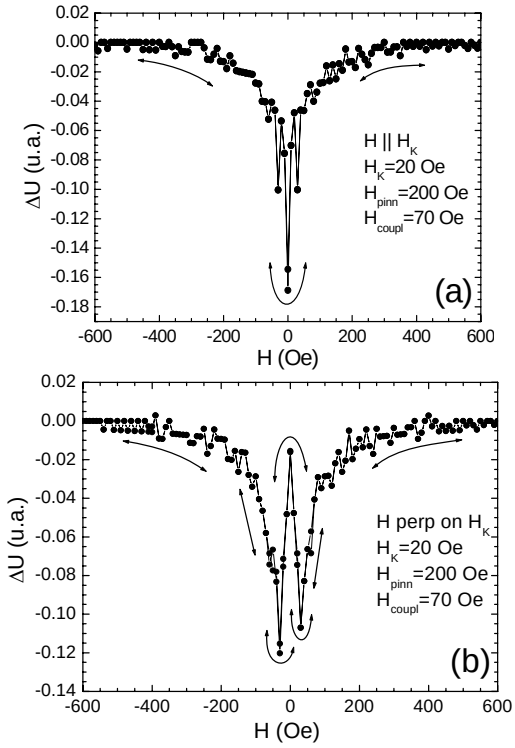

Fig. 9. The response of the system, presented in Fig. 8, when the easy axis of the GMR sensors is (a) parallel and (b) perpendicular to the applied magnetic field.

The measurement configuration presented above have the advantage of sharp and sy metric peaks around zero field at which the GMR sensors presents a maximum sensitivity. The particle detection will take place in low magnetic fields which means a smaller electrical current through the field generator strap and a lower temperature of the chip.

4. Conclusions

We presented in this paper some micromagnetic simulations regarding the use of the GMR sensors for biomedical applications such as rotation sensors and detection of magnetic particles labelled with biological systems that have to be investigated. The results of these simulations will be verified by experiments using the measurement systems that we designed and will be presented in other paper.

References

[1] G. Reiss, L. van Loyen, T. Lucinski, D. Elefant, H. Bruckl, N. Mattern, R. Rennekamp, W. Ernst, J. Magn. Magn. Mater. **184**, 281 (1998).
[2] John O. Oti in: SimulMag Version 1.0, Micromagnetic Simulation Software, User's Manual, Electromagnetic Technology Division, National Institute of Standards and Technology Boulder, Colorado 80303, December 1997.
[3] J. Schotter, P.B. Kamp, A. Becker, A. Pühler, G. Reiss, H. Brückl, Biosensors and Bioelectronics **19**, 1149 (2004)
[4] J. C. S. Kools, Th. G. S. M. Rijks, A. E. M. De Veirman, R. Coehoorn, IEEE Trans. Magn. **31**, 3918 (1995).

*Corresponding author: volmerm@unitbv.ro